

**INVESTIGATING LOCALIZATION PHENOMENA USING FINITE ELEMENT
AND MESHLESS METHODS**

by

David Masillamani Ponsingh

Department of Mechanical Engineering

APPROVED:

Jack Chessa, Ph. D., Chair

Arturo Bronson, Ph. D.

Michael Huerta, Ph. D.

Cesar Carrasco, Ph. D.

Charles H. Ambler, Ph. D.
Dean of Graduate School

PREVIEW

DEDICATED TO MY FAMILY

**INVESTIGATING LOCALIZATION PHENOMENA USING FINITE ELEMENT
AND MESHLESS METHODS**

by

DAVID MASILLAMANI PONSINGH

THESIS

Presented to the Faculty of the Graduate School of

The University of Texas at El Paso

in Partial Fulfillment

of the Requirements

for the Degree of

MASTER OF SCIENCE

Department of Mechanical Engineering

THE UNIVERSITY OF TEXAS AT EL PASO

DECEMBER 2004

UMI Number: 1423732

PREVIEW

UMI[®]

UMI Microform 1423732

Copyright 2005 by ProQuest Information and Learning Company.
All rights reserved. This microform edition is protected against
unauthorized copying under Title 17, United States Code.

ProQuest Information and Learning Company
300 North Zeeb Road
P.O. Box 1346
Ann Arbor, MI 48106-1346

ACKNOWLEDGEMENTS

I would like to express my sincere thanks to Dr. Jack Chessa for his valuable advice throughout my graduate studies and his support. I wish to thank him for teaching me how to take initiatives and work personally. His able guidance and vision helped in completion of the thesis.

My special thanks to FAST Center for Structural Integrity of Aerospace Systems sponsored by the National Institute of Standards and Technology for supporting me during summer 2003 semester.

My sincere thanks and appreciation to Dr. Michael Huerta, Dr. Cesar Carrasco, Dr. Arturo Bronson for serving on the committee at a short notice. I must thank Dr. Huerta for his advice during my studies and also for writing a recommendation letter. I also take this opportunity to acknowledge and thank my colleague and friend Javed Bilal Khan for his useful discussions and also for troubleshooting some of the problems I faced with the linux workstations. I dedicate this work to my beloved parents who have always supported me and encouraged me throughout my studies.

October 20, 2004.

ABSTRACT

This thesis investigates the validity of meshless methods and finite element methods in the investigation of strain localization phenomena in which is an important factor in many nonlinear solid mechanics problems. The term strain localization refers to the appearance of patterns of deformation that are restricted to narrow regions in the solid domain. Most often the deformation observed is that of shear, such a form of localization is referred to as a shear band. The thickness of typical shear bands for metals are approximately 10-30 μm which is typically orders of magnitude less than the dimensions of the specimen. Even with significant mesh refinement, it becomes difficult to observe this extremely small length scale with traditional numerical method.

Several benchmark problems are solved using traditional finite element methods and reproducing kernel particle method (RKPM) which is a particle meshless methods.. These problems include tensile instability of a bar, pressure instability in a cylindrical shell, and the Kalthoff Problem. In addition a variety of material laws were employed for each method and problem; some of which include J2 plasticity and thermo-viscoplasticity. Initially finite element analysis of a tensile bar is performed using strain softening material law to study localization phenomenon. Strain-softening is a decline of uniaxial stress at increasing strain or generally, where the tangent moduli ceases to be positive definite. Strain softening without a length scale results in the structure failing with a zero energy dissipation and the width of the shear band tends to become zero. In order to consider energy dissipation in the form of heat and also to incorporate a length scale in the problem, we study the same problem using a rate dependent material model namely thermo-viscoplastic constitutive law.

Meshless methods are a new class of computational modeling tools that have been proved to have better potential to study large deformation problems such as localization, extreme deformation, damage etc. Using meshless methods, the formation of multiple shear bands was observed at high strain rates. The behavior and propagation of dynamic shear bands were studied using meshless methods which were not feasible using conventional finite element method. Several examples are presented to show the efficacy of meshless methods to study strain localization problems. The organization of this Thesis is as follows: Chapter 1 gives an overview to the phenomena of strain localization as well as the general problem statement: Chapter 2 gives an overview of finite element methods and RKPM (the two methods studied): Chapter 3 illustrates the relative merits of various numerical solutions of strain localization phenomena by examples and Chapter 4 outlines a novel approach to modeling strain localization phenomena using enriched finite elements (X-FEM).

TABLE OF CONTENTS

Page No.

| | |
|--|-----|
| ACKNOWLEDGEMENTS..... | iv |
| ABSTRACT..... | v |
| TABLE OF CONTENTS..... | vii |
| LIST OF FIGURES..... | x |
| TABLES..... | xiv |
| CHAPTERS | |
| 1. REVIEW OF LOCALIZATION PHENOMENON | |
| 1.1 Introduction..... | 1 |
| 1.2 Problem Statement..... | 4 |
| 1.3 Localization Mechanism | |
| 1.3.1 Strain Gradient Plasticity..... | 10 |
| 1.3.2 Strain Softening..... | 12 |
| 1.3.4 Micro-damage..... | 13 |
| 1.3.5 Thermal Softening..... | 14 |
| 1.4 Constitutive Models | |
| 1.4.1 Hyperelasticity | 15 |
| 1.4.2 Strain Softening Plasticity..... | 16 |
| 1.4.3 Viscoplasticity..... | 17 |
| 1.4.4 Thermo-viscoplasticity..... | 18 |

| | |
|--|----|
| 1.4.4 Johnson and cook model..... | 20 |
| 1.7 Summary..... | 21 |
| 2. NUMERICAL METHODS | |
| 2.1 Introduction | |
| 2.11 Overview of the finite element method | 26 |
| 2.2 Meshless Methods | |
| 2.2.1 Smoothed Particle Hydrodynamics..... | 26 |
| 2.2.2 Reproducing Kernel Particle Method | 28 |
| 2.2.3 Element free Galerkin..... | 31 |
| 2.3 Conclusions..... | 33 |
| 3. EXAMPLE PROBLEMS | |
| 3.1 Introduction..... | 38 |
| 3.2 Tensile Instability..... | 40 |
| 3.3 Pressure Instability..... | 46 |
| 3.4 Kalthoff Problem..... | 51 |
| 3.5 Conclusions..... | 58 |
| 4. Orthogonal machining problem | |
| 4.1 Introduction..... | 61 |
| 4.3 Taguchi matrix for 2^3 factorial design..... | 63 |
| 4.4 Conclusions..... | 66 |

5. X-FEM - FUTURE WORK

| | |
|--|-----|
| 5.1 Introduction..... | 67 |
| 5.2 Overview of X-FEM Approximation..... | 68 |
| 5.3 Enrichment for Shear Bands..... | 69 |
| 5.4 Conclusions..... | 70 |
| REFERENCES..... | 71 |
| APPENDIX..... | 83 |
| CURRICULUM VITAE..... | 104 |

LIST OF FIGURES

Page No.

| | |
|--|----|
| Figure 1.1 Load applied and boundary conditions for Desrues and Viggiani, stereophotogrammetry experiment..... | 2 |
| Figure 1.2 Stereophotogrammetry images of shear strain intensity (top row) and volumetric strain intensity (bottom row) showing localization phenomena. The sequence of images represent shear strain intensity and volumetric strain intensity. (Desrues and Viggiani, 2004)..... | 3 |
| Figure 1.3 Computational domain of a body Ω with a line of strong discontinuity in the displacement field of Γ_c . The traction and displacement boundaries are denoted by Γ_t and Γ_u , respectively | 4 |
| Figure 1.4 Illustration of the 1-D problem solved in Belytschko et. al., (1986)..... | 7 |
| Figure 1.5 Stress strain curve used by Belytschko et al. 1986..... | 8 |
| Figure 1.6 Uniaxial stress-strain in a material exhibiting strain softening..... | 13 |
| Figure 1.7 Example of a stress strain curve for a thermal softening material | 15 |
| Figure 2.1 SPH particle neighborhood Libersky LD, Petschek AG (Libersky LD, Petschek AG , 1991)..... | 27 |
| Figure 2.2 FEM regular mesh and an equivalent meshless discontinuity..... | 30 |
| Figure 2.3 A 1-D RKPM shape function whose support spans seven nodes (Zhang et al. 2001)..... | 31 |

| | |
|---|----|
| Figure 3.1 A rectangular bar subjected to tensile forces..... | 37 |
| Figure 3.2 Modified stress strain curve with linear hardening for strain softening material law..... | 38 |
| Figure 3.3 Tensile instability using FEM with strain softening material law– coarse mesh..... | 39 |
| Figure 3.4 Tensile instability using FEM with strain softening material law– fine mesh | 41 |
| Figure 3.5 Tensile instability using FEM with strain softening material law– fine mesh; zoom view with mesh | 41 |
| Figure 3.6 Tensile instability using RKPM with strain softening material plot of effective plastic strain | 43 |
| Figure 3.7 Tensile instability problem using RKPM with thermo-viscoplastic material model , plot of effective plastic strain..... | 44 |
| Figure 3.8 Tensile instability problem using RKPM with thermo-viscoplastic material model..... | 44 |
| Figure 3.9 Computational domain and boundary conditions used to model pressure instability in a 2D hollow cylinder (quarter part shown in Figure)..... | 63 |
| Figure 3.10 Tensile instability using FEM with thermo-viscoplastic law, plot of temperature..... | 45 |
| Figure 3.11 Boundary conditions for pressure in a 2D hollow cylinder..... | 46 |
| Figure 3.12 Pressure instability using FEM with J2 plasticity material law, plot of effective plastic strain material law..... | 67 |

| | |
|--|----|
| Figure 3.13 Pressure instability using FEM with thermoviscoplastic law , plot of effective plastic strain..... | 48 |
| Figure 3.14 Pressure instability using FEM with thermo-viscoplastic law, plot of temperature..... | 49 |
| Figure 3.15 Results for the pressure instability problem using RKPM with J2 plasticity, plot of effective plastic strain..... | 50 |
| Figure 3.16 Results for the pressure instability problem using RKPM with thermo-viscoplastic model, plot of effective plastic strain..... | 50 |
| Figure 3.17 Results for the pressure instability problem using RKPM with thermo- viscoplastic model, plot of temperature..... | 51 |
| Figure 3.18 Kalthoff single notch problem of an impact loaded plate with a pre-notch..... | 52 |
| Figure 3.19 Velocity curve for the Kalthoff problem | 53 |
| Figure 3.20 The configuration of single notch specimen (Li and Liu, 2000)..... | 54 |
| Figure 3.21 Curved shear band formation (Zhou et al., 1996)..... | 54 |
| Figure 3.22 Curved shear band formation showing temperature, (Li et al., 2001).... | 54 |
| Figure 3.23 2D simulations of Kalthoff problem using FEM with thermo-viscoplastic model – plot of effective plastic strain..... | 55 |
| Figure 3.24 2D simulations of Kalthoff problem using RKPM with thermo-viscoplastic model – plot of effective plastic strain..... | 55 |

| | |
|---|----|
| Figure 3.25 2D simulations of Kalthoff problem using FEM with | |
| thermo-viscoplastic model – plot of temperature..... | 56 |
| Figure 3.26 2D simulations of Kalthoff problem using RKPM with | |
| thermo-viscoplastic model – plot of temperature..... | 56 |
| Figure 4.1 Finite element mesh of the tool and work piece..... | 63 |
| Figure 4.2 Contours of effective strain in orthogonal machining problem..... | 65 |
| Figure 4.3 Plot of effective strain in orthogonal machining | |
| problem, isosurfaces..... | 65 |
| Figure 5.1 Nodes that are enriched in X-FEM..... | 69 |

TABLES

Page No.

| | | |
|------------------|---|----|
| Table 3.1 | Material parameters and values for finite deformation J2 plasticity law.. | 38 |
| Table 3.2 | Material parameters and values for thermo-viscoplastic law..... | 38 |
| Table 3.3 | Material parameters and values for finite deformation J2 plasticity law.. | 47 |
| Table 3.4 | Material parameters and values for thermo-viscoplastic law..... | 53 |
| Table 4.1 | Taguchi matrix..... | 63 |

Chapter 1

REVIEW OF LOCALIZATION PHENOMENON

1.1 Introduction

Localization is the phenomena where a large degree of deformation occurs in highly concentrated regions. Most often the deformation observed is that of shear, such a form of localization is referred to as a shear band. These deformation patterns are associated with high displacement gradients. The discontinuous deformations that arise due to fracture are not considered here. The study of shear bands are important in a wide range of applications including high speed machining, high rate forming, explosive welding, armor penetration and vehicle crash-worthiness. At high strain rates, thermal softening occurs due to transfer of plastic work to local heating of the material. At high strain rates the heat transfer is negligible due to the disparate time scales of straining and thermal conductivity.

Strain localization is a common phenomenon in granular as well as ductile materials, and has been thoroughly analyzed both from experimental (Vardoulakis and Graf, B., 1985; Han and Drescher, 1993; Tatsuoka et al., 1990; Finno et al., 1997) and theoretical points of view (Schaeer, 1990; Schaeer and Shearer, 1997; Vardoulakis, Graf, 1985). From the experimental point of view, nucleation and growth of shear bands have been investigated under various testing conditions—for instance, a specific biaxial apparatus has been developed by Drescher et al., 1990. Also stereophotogrammetry has been used by Desrues et al., (Desrues et al., 1985) and Finno et al., (Finno et al., 1997). Other methods include X-ray radiography (Roscoe et al., 1963; Roscoe, 1970) and X-ray tomography (Desrues et al.,

1996). As a result many qualitative aspects of the physics of shear bands are well-documented (Gajo et al., 2004).

Figures 1.1 and 1.2 show experimental results from compression tests on sand carried out in Grenoble. Jacques Desrues and Gioacchino Viggiani (Desrues et al., 2004). In this experiment the researchers used a pressure cell and loading device to apply a uniform displacement at one end while keeping the other end of body fixed. They used a technique called stereophotogrammetry in which a series of photographs are viewed in stereo. The displaced regions appear elevated depending upon the magnitude of displacement so in Figures 1.1 and 1.2 the regions with enlarged pixels denote regions of high deformation. Using this data they were able to calculate the experimental strains.

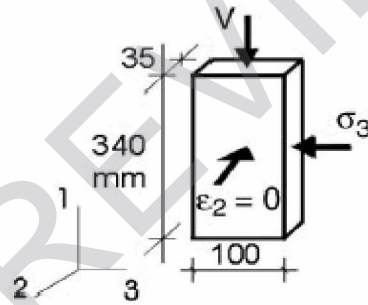


Figure 1.1 Applied load and boundary condition for compression test on sand specimens (Desrues and Viggiani, 2004).

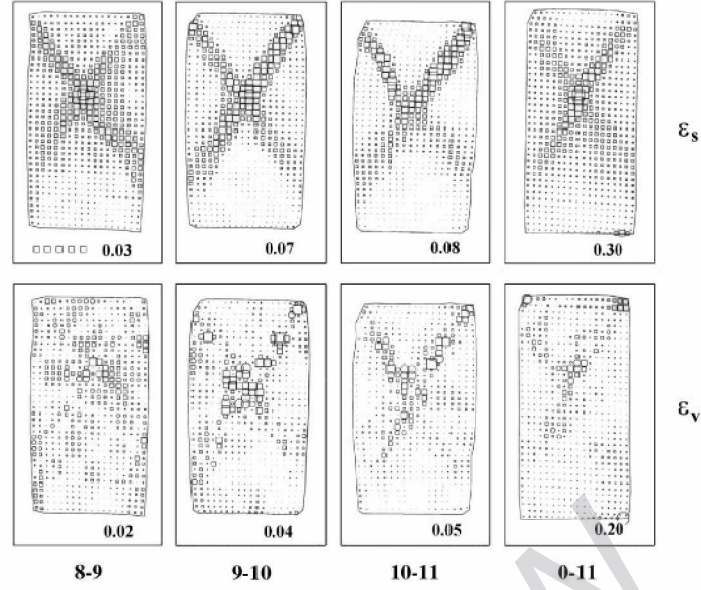


Figure 1.2 Sequence of stereophotogrammetry images of shear strain intensity (top row) and volumetric strain intensity (bottom row) showing localization phenomena. (Desrues and Viggiani, 2004).

Strain localization in solid mechanics involves a narrow region (“the localization band”) with a high displacement gradient ∇u across the width of the band. This condition is produced by a variety of constitutive models, such as elastoplastic or damage models, as long as they exhibit local material softening. As will be discussed in Section 1.4 material softening results in material instability which localizes all the strain energy to a small region. This phenomena poses considerable difficulties in numerical solutions due to severe mesh dependency. Some of the approaches to capture the shear band are to use standard continuous elements, adaptive finite elements and enhancing the displacement field with enrichment functions so that the true slip line can be captured.

Li et al. (Li et al., 2001) used a meshfree Galerkin simulation of dynamic shear band propagation in an impact-loaded pre-notched plate (Kalthoff’s problem with single

notch) in both two and three dimensions. The ductile-to-brittle failure mode transition was observed in their numerical simulations. Also they were able to capture dynamic shear bands and study the microstructure of shear bands. Belytschko and Tabbara (Belytschko and Tabbara, 1996) used the element free Galerkin (EFG) method to simulate the Kalthoff's double notch experiment.

1.2 Problem Statement

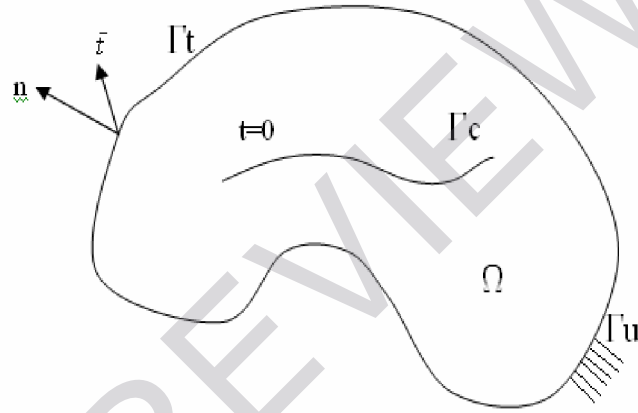


Figure 1.3: Computational domain of a body Ω with a line of strong discontinuity in the displacement field of Γ_c . The traction and displacement boundaries are denoted by Γ_t and Γ_u , respectively.

Consider a multiply connected domain Ω , bounded by Γ as shown in Figure 1.3. The boundary is partitioned into three sets Γ_u , Γ_t and Γ_c . Displacements are prescribed on Γ_u and the tractions are prescribed on Γ_t . Γ_c is a line of strong discontinuity idealizing the highly localized weak discontinuity in the displacement field of a localization phenomena. The governing equations are conservation of linear momentum, conservation of mass and conservation of energy on Ω .

The conservation of linear momentum in updated lagrangian form is as follows:

$$\rho \dot{u}_i = \sigma_{ij,j} + b_i \quad \text{in } \Omega$$

where ρ is the density in current configurations, σ is the Cauchy stress tensor, u is the displacement field, and b is the associated body force. In the above and in all subsequent equations a repeated index implies a summation and all the indices with respect to the current configuration. All fields are expressed in terms of reference on material coordinates.

The conservation of mass is

$$\rho = \frac{1}{J} \rho_o \quad (1.2)$$

where J is the Jacobian of the deformation from the reference to the current configuration and ρ_0 is the density in the reference configuration. The conservation of energy is expressed as follows:

$$\rho \dot{w}^{\text{int}} = D_{ij} \sigma_{ij} - q_{ij} + \rho \mathcal{S} \quad (1.3)$$

where w^{int} is the internal energy per unit mass, D_{ij} is the deformation rate defined as

$$D_{ij} = \frac{1}{2} (\dot{u}_{i,j} + \dot{u}_{j,i}) \quad (1.4)$$

q_i is the heat flux and \mathcal{S} is the heat source. In addition to the above governing equations the

following constitutive equations are required

$$\sigma_{ij}^{\nabla} = C_{ijkl}^{\sigma \nabla} D_{kl} \quad (1.5)$$

where σ_{ij}^{∇} indicates an objective rate of the Cauchy stress such as the Jaumann, Truesdell or Green-Naghdi rates, and $C_{ijkl}^{\sigma \nabla}$ is the associated material stiffness tensor relating the objective rate to the rate of deformation tensor D. For completeness we give the Jaumann objective rate.

$$\sigma_{ij}^{\sigma \nabla} = \frac{D}{Dt} \sigma_{ij} - W_{ij} \sigma_{kj} - \sigma_{ik} W_{jk} \quad (1.6)$$

where W_{ij} is the spin tensor defined as;

$$W_{ij} = \frac{1}{2} (\dot{u}_{i,j} - \dot{u}_{j,i}) \quad (1.7)$$

The traction boundary conditions are given by

$$n_j \sigma_{ji} = \bar{t}_i \quad (1.8)$$

where n_j is the outward normal to Ω as shown in Figure 1.3 and t_i is the prescribed traction. The displacement boundary conditions are given by

$$u_i = \bar{u}_i \quad \text{on} \quad \Gamma_u \quad (1.9)$$

where \bar{u} is the prescribed displacement.

Since the equations of motion are second order in time, initial conditions on the displacements and velocities are needed.

$$u_i(\mathbf{x}, t = 0) = u_i^o(\mathbf{x}) \quad \forall \mathbf{x} \in \Omega \quad (1.10)$$

$$\dot{u}_i(\mathbf{x}, t = 0) = v_i^o(\mathbf{x}) \quad \forall \mathbf{x} \in \Omega \quad (1.11)$$

1.3 Localization Mechanisms

The problem of strain localization has been studied by many researchers. Bazant and Belytschko, (Bazant and Belytschko., 1985) gave analytical solutions to a 1D localization problem involving tensile wave propagation in a bar of bilinear elastic material; while not very realistic physically it gives excellent insight into the phenomenon of localization and the associated mesh sensitivity. They considered a finite homogenous bar $\Omega = (L, -L)$ with constant cross section A and density ρ , initially at rest as shown in Figure 1.4. A constant traction is applied at both ends $x = \pm L$, as shown for a bilinear elastic curve in Figure 1.5. This simplified model exhibits localization due to the fact that the tangent modulus of the second portion of the curve is negative. The stress and strain at which the tangent modulus becomes negative is given by S_e and ε_p , respectively. The traction at the ends is chosen such that $0.5 S_e < S_o < S_e$.

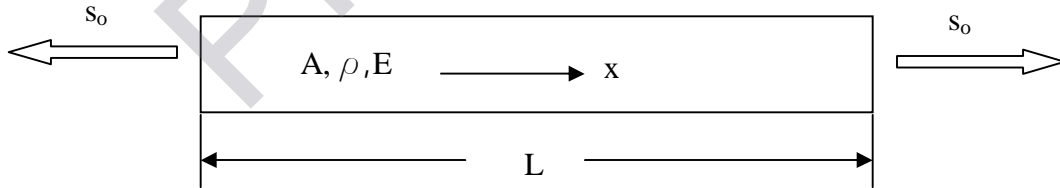


Figure 1.4 Illustration of the 1-D problem solved in Bazant and Belytschko., 1985.

Initially an elastic stress wave propagates from both end. The two elastic waves interfere constructively at the midpoint causing the stress amplitude to double and exceed S_e .

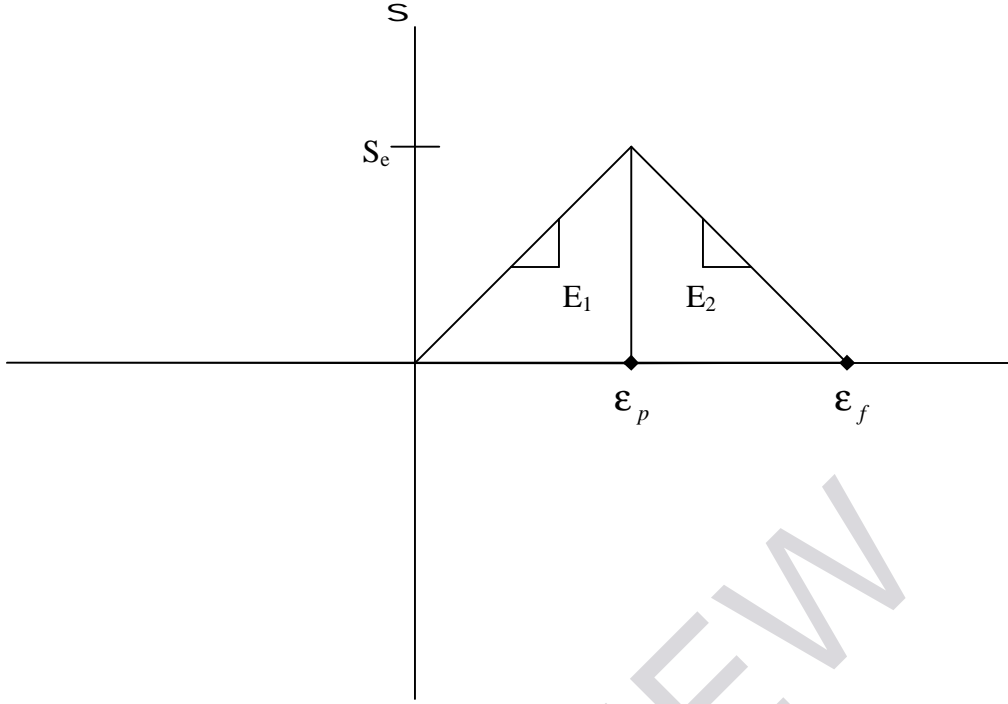


Figure 1.5 Stress strain curve used by Bazant and Belytschko (Bazant and Belytschko., 1985).

In 1D the conservation of momentum equation (1.1) reduces to the linear wave equation as follows:

$$\frac{\partial^2 u}{\partial t^2} = c^2 \frac{\partial^2 u}{\partial x^2} \quad (1.12)$$

where c is the wave speed given by

$$c = \sqrt{\frac{E}{\rho}} \quad (1.13)$$

When the stress in the bar is less than S_e the tangent modulus is positive and the wave speed is real. This case results in (1.10) being hyperbolic in nature. When the stress in the bar exceeds S_e the tangent modulus is negative and the wave speed becomes imaginary and (1.10) is elliptic in nature. The fact that waves cannot propagate at a finite speed in an

elliptic system causes all the strain energy to be trapped which further softens the material in a feedback type instability. It should be noted that the tangent modulus losing positive definiteness coincides with the onset of strain softening. According to Belytschko et al., (Belytschko et al., 1986) mesh refinement causes the solution to rapidly converge to a Dirac function where the localization occurs on a width of zero thickness; this is often referred to as a set of measure zero.

When such problem is studied using finite elements the localization is narrowed to the width of one element. So, as the mesh is refined the width of the numerical localization is reduced by an equal amount. No matter how small the mesh becomes the width of the localization will not converge. This phenomena is referred to as mesh sensitivity, and is the bane of many numerical schemes.

The final energy dissipated in the process vanishes, indicating the non-physical nature of the solution. Bažant and Belytschko observed that this fact is due to plastic (softening) zone is of length zero. In the later approaches they came up with regularization approaches that involve introduction of length scale in the material model, which they referred to as localization limiters. In a similar paper Bažant and Belytschko (Bažant and Belytschko., 1985) studied strain softening in a hollow sphere caused by a uniform normal traction at the exterior.

Needleman (Needleman, 1988) studied the role of material rate dependence and mesh sensitivity in localization problems. Needleman shows that material rate dependence implicitly introduces a length scale into the governing equations, even though the constitutive description does not contain an explicit length scale. For rate independent materials, strain localization is associated with loss of hyperbolicity of equilibrium of the momentum